Chin. J. Astron. Astrophys. Vol. 6 (2006), No. 2, 247–259
(*http://www.chjaa.org*)

Chinese Journal of
Astronomy and
Astrophysics

Transequatorial Filament Eruption and Its Link to a Coronal Mass Ejection *

Jing-Xiu Wang[1,2], Gui-Ping Zhou[1], Ya-Yuan Wen[1], Yu-Zong Zhang[1], Hua-Ning Wang[1], Yuan-Yong Deng[1], Jun Zhang[1] and Louise K. Harra[2,1]

[1] National Astronomical Observatories, Chinese Academy of Sciences, Beijing 100012; *wangjx@ourstar.bao.ac.cn*
[2] Mullard Space Science Laboratory, University College London, Holmbury St Mary, Dorking, Surrey, RH5 6NT, UK

Received 2005 August 1; accepted 2005 December 6

Abstract We revisit the Bastille Day flare/CME Event of 2000 July 14, and demonstrate that this flare/CME event is not related to only one single active region (AR). Activation and eruption of a huge transequatorial filament are seen to precede the simultaneous filament eruption and flare in the source active region, NOAA AR 9077, and the full halo-CME in the high corona. Evidence of reconfiguration of large-scale magnetic structures related to the event is illustrated by SOHO EIT and Yohkoh SXT observations, as well as, the reconstructed 3D magnetic lines of force based on the force-free assumption. We suggest that the AR filament in AR 9077 was connected to the transequatorial filament. The large-scale magnetic composition related to the transequatorial filament and its sheared magnetic arcade appears to be an essential part of the CME parent magnetic structure. Estimations show that the filament-arcade system has enough magnetic helicity to account for the helicity carried by the related CMEs. In addition, rather global magnetic connectivity, covering almost all the visible range in longitude and a huge span in latitude on the Sun, is implied by the Nançay Radioheliograph (NRH) observations. The analysis of the Bastille Day event suggests that although the triggering of a global CME might take place in an AR, a much larger scale magnetic composition seems to be the source of the ejected magnetic flux, helicity and plasma. The Bastille Day event is the first described example in the literature, in which a transequatorial filament activity appears to play a key role in a global CME. Many tens of halo-CME are found to be associated with transequatorial filaments and their magnetic environment.

Key words: Sun: corona – Sun: coronal mass ejections (CMEs) – Sun: activity – Sun: magnetic fields

1 INTRODUCTION

There is a hierarchy of solar activity, ranking from the ubiquitous small-scale activity on the quiet Sun, to that in active regions (ARs), and to the large and more global scale activity, e.g., coronal mass ejections (CMEs). Each level of activity is believed to be hosted by a class of magnetic

* Supported by the National Natural Science Foundation of China.

structures. Moreover, the magnetic structures, themselves, may form a hierarchy in solar magnetism too.

The interplay of intranetwork magnetic elements, network fields and ephemeral regions is the ultimate source of small-scale activity in the form of minifilament eruptions, macrospicules and microflares on the quiet Sun (Wang et al. 2000; Zhang et al. 2000). Ephemeral active regions that represent the small-scale end of the AR spectrum (Harvey & Martin 1973; Martin 1988), may also play a role in active-region scale activity as well. However, the key components of magnetic fields in active regions are sunspot, plage (enhanced network), and newly emerging flux in the forms of emerging flux regions (EFRs) and/or moving magnetic features (MMFs). Although the nature of small-scale MMFs are not well known, they are likely to belong to the strong magnetic field of ARs.

Although each level of activity results from an interaction of magnetic structures with different scales which may come from different levels of the solar magnetic hierarchy, there is always a basic magnetic component which specifies the scale of the activity. For example, the network magnetic fields seem to determine the scale of quiet sun activity, e.g., microflares and minifilaments; while the sunspot fields appear to specify the scale of flares and AR filaments. *A natural question is whether or not there is a magnetic component, which may represent a larger, more global scale in the solar magnetic hierarchy which is related to CMEs.* This is a key question for a satisfactory understanding of solar magnetic activity (Parker 2001).

For a long time solar astronomers have been mostly concentrating their efforts on the structure and evolution of ARs and small-scale magnetic elements on the quiet Sun. Early magnetographs were developed for AR observations aimed at understanding magnetism in flares. Later, improvement in sensitivity and resolution of magnetographs provided the resolution necessary for observing small-scale magnetic fields on the quiet Sun. The limited field of view obtained by these instruments contains no apparent information of large-scale magnetic structures. Even in full disk magnetograms, which contain information on large-scale field structures, the crowded small-scale magnetic elements (known as *'salt and pepper'*) related to small low-lying loops would make the recognition of coherent large-scale magnetic structures difficult. Therefore, so far, it is not known if there is an intrinsic large-scale component of solar magnetism which could be responsible for more global solar activity, e.g. CMEs. To explore the possible large-scale magnetic component, which may be related to the CME parent, is the primary motivation of this work.

In this paper, the term *CME parent magnetic structure* is used to describe a large-scale magnetic composition, whose magnetic flux and frozen-in plasma becomes a CME when erupted. The CME parent magnetic structure characterizes the pre-CME magnetic configuration. In solar literature, the term of *CME source region* is widely used (Harrison 1990), but it often loosely refers to the surface activity and/or an observed quiet or active region which was observed to be associated with a CME. Thus, the so-called CME source region is adopted by the literature in the sense that it represents a part of the CME parent magnetic structure, in which the initial opening of the CME parent structure (Švestka 2001) and the CME-associated surface activity took place.

Using the Bastille Day event as an example, we demonstrate for the first time that a transequatorial filament and its sheared magnetic arcades are part of a large-scale magnetic structure which is CME-prolific. In the next section, we review the Bastille day event, and point out that one fact about the event has been missed in all published literature – the pre-CME activation and eruption of a huge transequatorial filament. In Section 2, we describe in detail the activity of the transequatorial filament which preceded the flare/CME event. In Section 3, we show evidence of reconfiguration of large-scale magnetic fields in associated with the rather global activity. In the discussion of Section 4 we suggest that the transequatorial filament and its sheared magnetic arcades may provide enough magnetic helicity for the CME. In the last section we draw the conclusions.

2 A BRIEF REVIEW OF BASTILLE DAY EVENT

The Bastille Day event is one of the most important active events in this solar cycle. This major event was characterized by an almost simultaneous filament eruption, flare onset and CME initiation. It is spectacular due to the intense X-ray emission, extremely high proton flux, and great geo-effects (see Topical Issue on the 2000 Bastille Day Flare Event, Solar Physics, Vol.204/1-2, 2001). For this Earth-directed CME, NOAA AR 9077 has been identified to be the source region.

Vector magnetograms of this active region were obtained by Huairou Solar Observing Station of the National Astronomical Observatories of Chinese Academy of Sciences (Deng et al. 2001).

The left panel of Figure 1 shows a LASCO (Large Angle and Spectrometric Coronagraph Experiment, Brueckner et al. 1995) C2 image of this earth-directed CME, showing internally twisted and linked structures spanning 360 degrees outside of the solar disk. In the right panel, a full-disc Hα filtergram, on which each AR was denoted by its NOAA numbers, is shown. Although AR 9077 was a large, superactive region, it is still too small to account for the global scale of the CME. Thus, this event may provide a good example to exemplify what type of large scale magnetic structure is involved in the CME process and fundamental to CME initiation. A brief summary on the observational results of the Bastille Day event is described below:

(1) Full halo-CME with complicated internal structures (Andrews 2001);
(2) Abrupt cessation of Type I and Type III metric storm (Reiner 2001; Chertok 2001; Wen et al. 2005) right before the event at widely separated sites (Maia et al. 2001);
(3) In the source region, AR 9077, fast sunspot motions, evidence of photospheric magnetic reconnection, great magnetic nonpotentiality and its obvious changes in the course of the filament eruption and explosive flare of significance, X5.7/3B (Zhang et al. 2001; Deng et al. 2001; Liu & Zhang 2001, 2002; Tian et al. 2002);
(4) Globalness of coronal radio emission and involvement of multiple flux systems; indications of electron event related to large-scale magnetic reconfiguration in the lower corona (Masuda, Kosugi & Hudson 2001; Maia et al. 2001);
(5) Effectiveness in influencing the geo- and helio-space (Raeder et al. 2001).

Several of the above facts seem to imply that the Bastille Day event is not solely an active region phenomenon, but involves a large-scale magnetic structure. This large-scale field composition may account for the continuous metric Type I and Type III storms in the pre-CME phase and the abrupt cessation right before the CME, and the multiple particle acceleration sites and global radio emission during the CME. Since the noise storms appear across the solar disk, it may also illustrate the global nature of the CMEs that are observed in LASCO C2 and C3 images. The strong and complex magnetic fields in AR 9077 played an important role in interacting with some large-scale field component that resulted in halo CMEs.

In a re-examination of observations, Wang and his co-workers (Wang 2002; Wang et al. 2005) recognized that one fact has been missing in the published literature: the pre-CME activation and eruption of a huge transequatorial filament. The AR filament in AR 9077 could be considered as the extension, or the rooting end of this huge filament. This paper is devoted to a detailed description of the transequatorial filament and its possible role in the global CME on the Bastille Day.

3 ACTIVITY OF THE TRANSEQUATORIAL FILAMENT

An huge transequatorial filament was mapped by the Huairou full disk Hα filtergraph equipped with a 2k×2k CCD. Figure 2 shows the filament compared with the background magnetic field from MDI (the Michelson Doppler Imager, Scherrer et al. 1995) magnetogram and coronal structures in SOHO EIT (the Extreme Ultraviolet Imaging Telescope, Delaboudinière et al. 1995) and Yohkoh SXT (Soft X-ray Telescope, Tsuneta et al. 1991) images. Basically the huge filament lies along an extended bipolar region (EBR) of generally low flux density in the full-disk magnetograms (Zhou et al. 2005). Magnetic fluxes of AR 9077 and several other smaller ARs, such as AR 9081, 9082 and 9084, etc., comprise part of the EBR. The active region filaments in AR 9077 and 9082 merged with the transequatorial filament from north and south, respectively, to form very long filament channels (see the dashed lines in the figure). Arcades above the filament (marked by arrows) which depicted the large-scale magnetic lines of force are seen in both EIT and SXT images. The soft X-ray arcades and the curved bright core in AR 9077 give a disc view of the 3-dimensional magnetic structure, as well as the three components in the classical flare/CME model. Besides the arcades associated with the transequatorial filament, there is another set of arcades extending from the south-west of AR 9077.

The filament activity is shown in the time sequence of Huairou Hα filtergrams in Figure 3a and 3b. The filament is often twisted, knotted, and kinked. A relaxation (e.g. disappearance of a

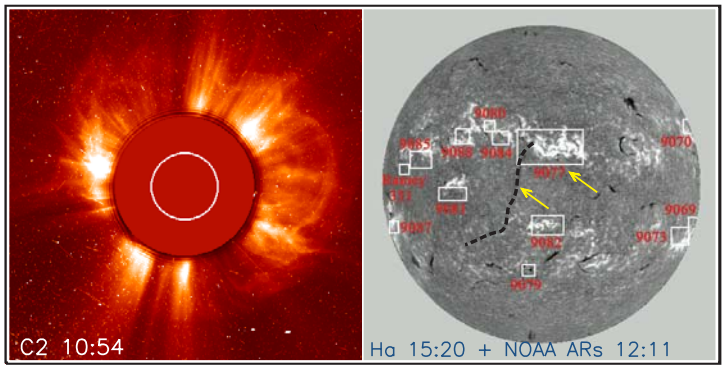

Fig. 1 Left: LASCO C2 image showing the Bastille CME on 2000 July 14, at 10:54 UT. Seen are internally linked and braided complex structures. Right: the NOAA numbers of Ramey sunspot at 12:11 UT are overlaid on an Hα image at 15:20 UT showing the CME's source regions as indicated by the two arrows. The dashed line marks the eruptive transequatorial filament associated with the CME.

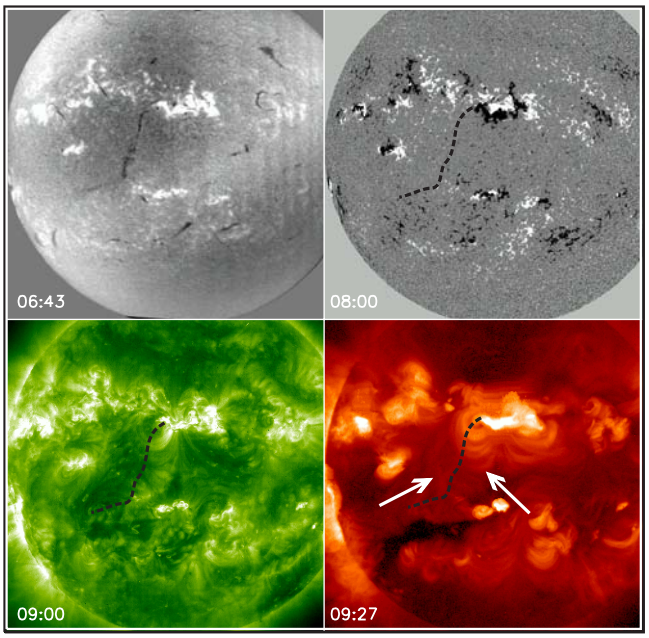

Fig. 2 A Huairou Hα filtergram (upper-left) shows a huge transequatorial filament, to which active region filaments in AR 9077 and AR 9082 are joined. The dashed lines in the other three panels mark the transequatorial filament. Arcades straddling the huge filament are seen clearly in an SOHO EIT 195 Å image (lower-left) as well as in a Yohkoh SXT image (lower right, see arrows). Magnetic flux distribution is shown by the SOHO MDI magnetogram (upper-right).

knot) was always observed shortly after each twist, kink or knot (see the arrows in the figure). For example, at 05:22 UT, the filament twisted into four knots, and a relaxation was seen at 06:22 UT (see also the twist and relaxation pairs from the images of 06:02–06:42, 07:22–08:02, and 09:02–09:42 UT). Disturbances started from the small filament in AR 9082 were transferred by the huge filament and propagated into AR 9077. The global eruption of the transequatorial filament

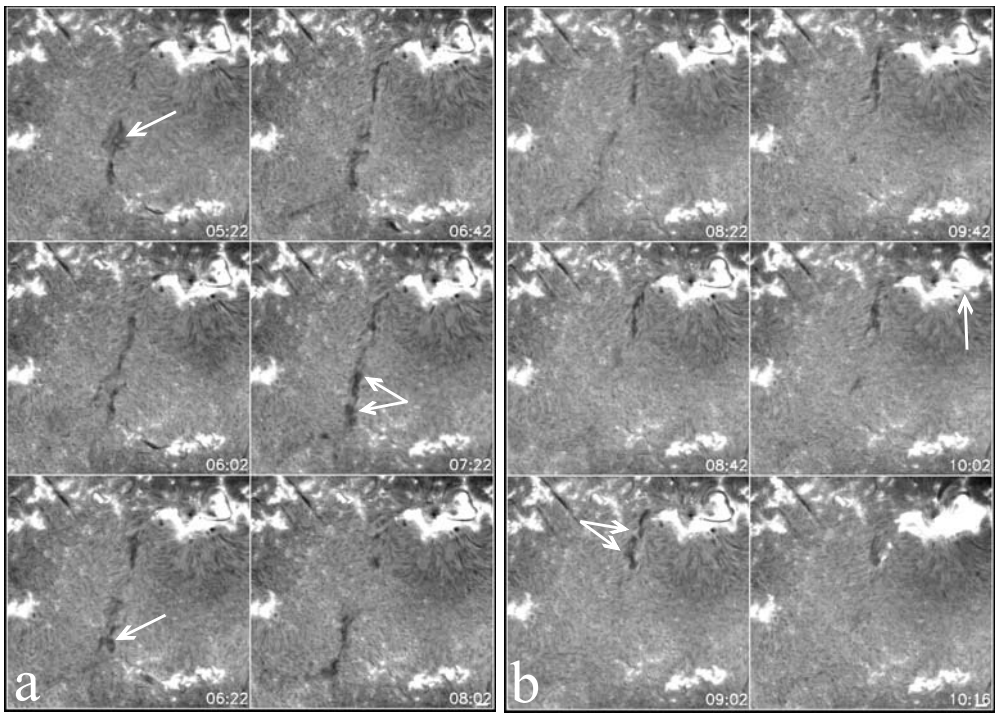

Fig. 3 Panels a, b: time sequence of Hα filtergrams showing the activation and eruption of the transequatorial filament. Arrows indicate the transequatorial filament and active region filament.

started approximately from 08:22 UT, 1 hour after the ejection of the AR filament in AR 9082; the braided brighter and darker threads in the huge filament were very clear at 09:02 UT when the filament became twisted close to its northern end; at the same time the filament in AR 9077 became activated. The filament in AR 9077 began to break out at approximate 10:02 UT, 1 hour after the activation of the transequatorial filament, at the same time as the earliest brightening of the Bastille day flare. The site of the first part of the AR filament to erupt is marked by an arrow in the image at 10:02 UT when the transequatorial filament only showed its remnants in eruption. The TRACE 195 Å movies showed that the main eruption of the filament in AR 9077 took place roughly from 10:10 UT. The transequatorial filament completely disappeared after 10:16 UT when the Bastille day flare/CME had already started (Zhang et al. 2001; Deng et al. 2001).

The activity in the transequatorial filament was also shown by the time sequence of EIT running difference (RD) images in Figure 4. These RD images are obtained by an EIT 195 Å image subtracted from the subsequent image. The darkening or brightening in the RD images indicates the movement of the associated surface activity. It is noticeable that the arcades above the filament showed incessant activity in the form of expansion and partial eruption, as well as the eruption of the transequatorial filament. Sometimes, the filament showed internal thread relaxing and rotating during the activation. This is very similar to that seen in AR filaments (Wang, Shi & Martin 1996). Typical examples are seen in the images at 01:26, 03:36, 06:00, and 08:00 UT on July 14. The filament appeared as a magnetic flux rope, while the filament threads resembled magnetic lines of force. At 03:36 UT the filament became extended and even wider than the whole AR 9077.

The selected RD images from 08:00 to 10:12 UT in the figure clearly show the propagation of a major disturbance of the transequatorial filament starting from the filament in AR 9082 to AR 9077. The three arrows at the image of 09:36 UT mark the positions of the most disturbed part of the filament at 08:36, 09:24 and 09:36 UT, respectively, from which the propagation direction of the disturbance is indicated. The AR 9077 flares were seemingly in response to the arrival of the

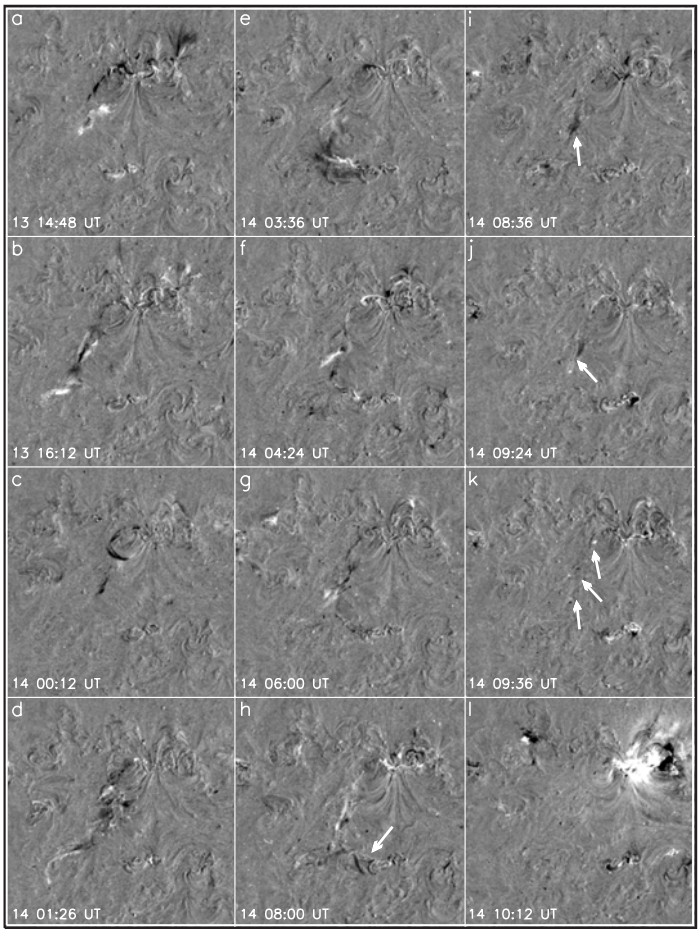

Fig. 4 Time sequence of EIT 195 Å Running Difference Images showing the filament's activation before the Bastille Day flare/CME. A few images exhibited the internal twisted threads of the filament. The arcades were in incessant activity in the form of expansion, brightening, and partial eruption.

disturbance of the huge filament. Such a major disturbance seems to be the key process leading to the Bastille Day flare/CME event. By 10:12 UT the transequatorial filament had disappeared completely.

4 RECONFIGURATION OF LARGE-SCALE MAGNETIC STRUCTURE

A reconfiguration of the large-scale magnetic structure after the major flare/CME event can be seen clearly by comparing the EIT and SXT images taken right before and well after the event. The primary changes are shown in Figure 5. First, the arcades straddling over the transequatorial filament disappeared; secondly, there appeared to be a dimming at both EUV and soft X-ray wavelengths. The dimming appeared at different, widely separated locations marked by the numbers '1', '2', and '3' in the figure. Areas '1' and '2' were newly dimmed regions. Region '3' was dimmed before but the dimming was enhanced after the Bastille Day event. The dimming was not a transient phenomenon but manifested itself as a long-term restructuring of the Sun's magnetic fields. We have tried to identify when this permanent restructuring, or the transient coronal holes took place. However, the 'snow storms' in the CCD detectors, caused by the impacting of high

energy particles make it impossible to observe the detailed evolution of the large-scale structures. It can not be dismissed that the long-term dimming illustrated in Figure 5 was not only caused by the Bastille Day event, but also by other two strong bursts roughly at 12:50 and 13:48 UT, respectively, identified from Nançay radioheliograms (Maia et al. 2001). The reconfiguration might be due to several flares and CMEs that occurred on the Bastille Day.

The widely separated dimmings shown in Figure 5 seem to imply that not only AR 9077, but also the multiple flux systems covering a broad spatial range are involved in the physical process which led to the major activity. To show this more clearly we have superposed the contours of intensity depletion in EIT base difference (BD) image, created from EIT images of 11:00–08:48 UT, on the top of a full disc MDI magnetogram taken at the closest time in Figure 6. The intensity depletion levels are 10% and 20% of the average intensity in the pre-event EIT image at 08:48 UT. Unlike the long-term dimming shown in Figure 5, the dimming in Figure 6 was transient and intrinsically related to the Bastille Day flare/CME.

The dimming contours on the disc showed a clearly bipolar form. EUV dimming observations have shown evidence that they are open field regions which were previously closed before the CME onset (Harra & Sterling 2003). We suggest that the depletion areas represent the footpoints of previously closed EBR. The most extensive dimming is associated with the transequatorial filament and AR 9077. It is located on both sides of the magnetic neutral zone of the EBR, which is outlined by the red, thick dashed lines. The other two strong dimming areas in the north-west and south-west (partially coincident with the radio emissions shown by Maia et al. 2001 and Wen et al. 2005) are of bipolar nature too. The south-west dimming is co-spatial with another extended bipolar region (EBR). We tentatively draw the magnetic neutral lines for this EBR. We speculate that for the Bastille Day flare/CME, at least, the above three bipolar regions were involved and partially erupted in the flare/CME process. The Bastille Day flare/CME is obviously not a single active region phenomenon.

The above optical observations are strongly supported by Nançay Radioheliograph (NRH) observations. Selected NRH images at 164 MHz are shown in Figure 7 from the pre-event Type I storm to the burst sources accompanying the expansion of the CME. Comparing Figure 7 with Figures 2, 5, and 6, we can identify the optical counterparts of the successively appearing radio sources which mainly corresponded to AR 9077 and AR 9082, two sets of magnetic arcades, transequatorial filament, and the other two bipolar regions, respectively. The direct imaging of the non-thermal electrons in the corona at metric wavelengths by NRH shows an even more complicated picture. Multiple magnetic flux systems which represent global magnetic connectivity were involved in the CME development. They show different spatial scales and cover almost all the visible range of longitude and a huge span in latitude. A CME model with a simple bipolar configuration can never match what has been observed in this and many other complex events.

To understand the gross 3-dimensional magnetic structures and their changes, associated with the activity of the transequatorial filament, we have made a non-linear force-free extrapolations (Yan & Sakurai 2000; Wang, Yan & Sakurai 2001) based on the MDI observations at 09:36 UT of July 14 and 16:03 UT of July 15, respectively. The reconstructed magnetic lines of force are superposed on the observed magnetograms and shown in Figure 8. The side view of the reconstructed magnetic lines of force is illustrated in Figure 9. The extrapolations are made by a two-step procedure. First, a linear force-free extrapolation was made based on the line-of-sight magnetic fields obtained by MDI. In this procedure the force-free coefficient, α, is chosen to have the extrapolated lines of force fit the intensity structures in the Hα, EUV and X-ray images. Secondly, the force-free extrapolation (Yan & Sakurai 2000) was further based on the vector fields whose transverse components were taken from the linear force-free extrapolation in the first step, while the line-of-sight component was directly taken from the MDI magnetograms.

The magnetic arcades overlying the transequatorial filament delineated by the intensity structures in the EIT and SXT images in Figure 2, are outlined by the magnetic lines connecting the opposite polarity flux on both sides of the EBR. The negative flux in AR 9077 has a large spatial extent, partially connecting a widely separated south-eastern AR, AR 9081, in the southern hemisphere and the enhanced positive network of the EBR. A few lines of force above the transequatorial filament, which connected the negative flux of AR 9077 and the positive flux in AR 9081 are sigmoidal with a reversed 'S' shape. Therefore, although a large-scale magnetic composition appears

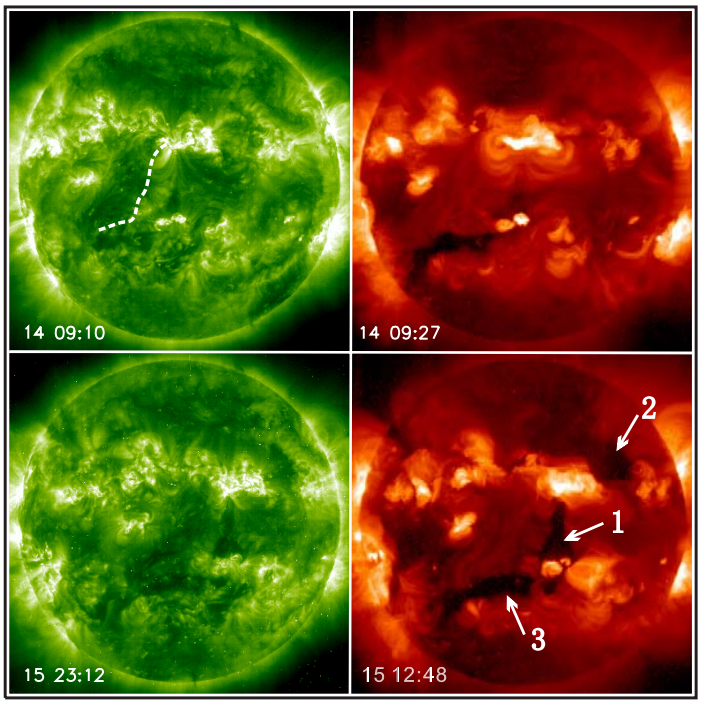

Fig. 5 Comparison of EIT 195 Å and SXT images right before and well after the Bastille Day flare/CME. The associated eruptive transequatorial filament is marked by a dashed line in an EIT 195 Å image (upper-left). Areas denoted by numbers '1'and '2' are long-term dimmings, and number '3' indicates an enhanced dimming.

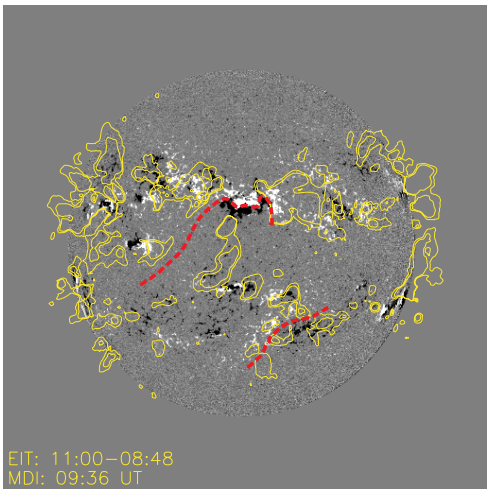

Fig. 6 Contours of EUV dimming deduced from EIT 195 Å image pair at 11:00 and 08:48 UT are superposed on an MDI magnetogram at 09:36 UT. The depletion levels are 10% and 20% of the intensity in undisturbed transition regions. Magnetic neutral lines are drawn to indicate the bipolar nature of the dimming.

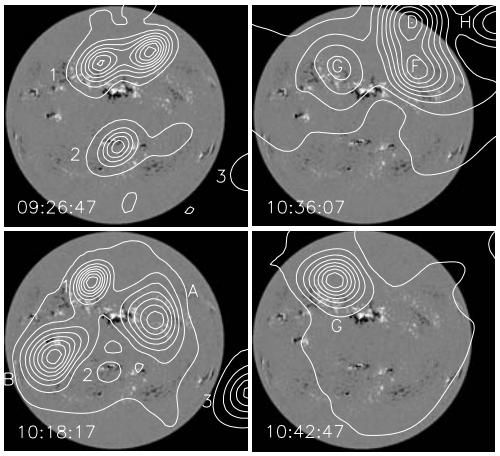

Fig. 7 Radio emission sources at 164 MHz obtained from NRH superposed on the MDI magnetograms at the closest time. Pre-event Type I storm sources are numbered as '1', '2', '3', and burst sources are denoted by capital letters. They encompassed almost the entire range of longitude and a huge span of longitude, which indicate that multiple-flux systems were involved in the CME development. The angular resolution of the NRH is $5.5' \times 3.2'$ at 164 MHz.

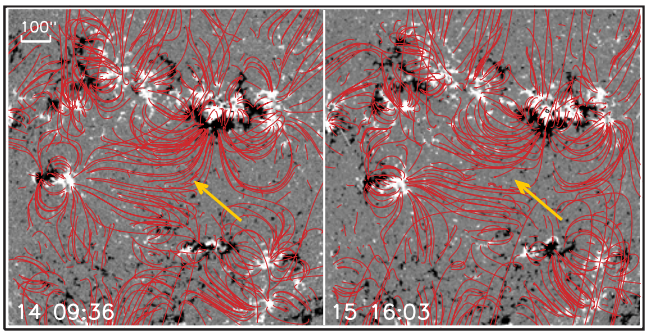

Fig. 8 Magnetic lines of force, reconstructed from non-linear force-free field extrapolation, are drawn on top of related MDI magnetograms before and after the Bastille Day flare/CME. Reconfiguration can be seen by comparing the force line structures. The scale is indicated in the left panel.

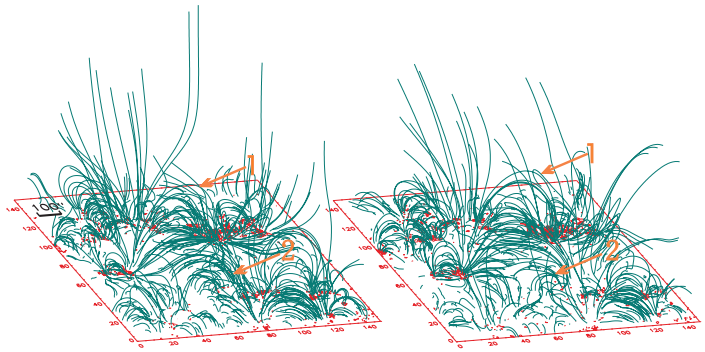

Fig. 9 Side view of the reconstructed 3-D magnetic structures shown in Fig. 8. The scale is indicated in the left panel.

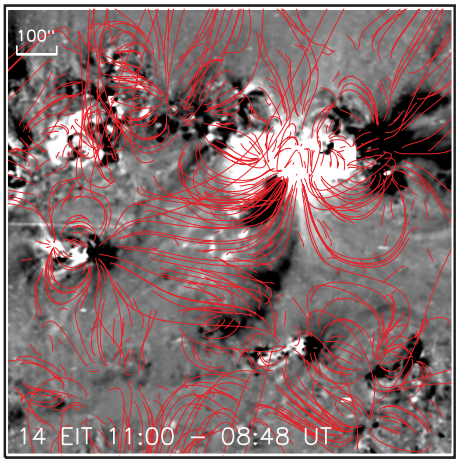

Fig. 10 EUV dimming shown by an EIT 195 Å BD image of 11:00–08:48 UT superposed with the reconstructed magnetic lines of force. The scale is indicated in the upper-left corner.

to be responsible for the global nature of the CME, the important role of the strong and highly non-potential magnetic fields in AR 9077 can not be ignored. There are also field lines, extending to very high altitude or already opened before the outburst of the flare/CME. Unfortunately, the 3-D reconstruction of magnetic lines of force does not give any indication about the magnetic field within the huge transequatorial filament. The general structure associated with the transequatorial filament is the magnetic arcades and some opening field lines that are rooted in the vicinity of the arcade footpoints. In Figure 9 the arcades are illustrated more clearly. Scrutinizing the reconstructed 3-d structures before and well-after the Bastille Day event, we find partial opening of the previously closed magnetic lines of force. Most of the sigmoidal lines of force have disappeared. More opening lines are seen from AR 9077 and 9082 after the activity. Arcades can still be seen at 16:03 UT on July 15, but at a more elevated location (see the two arrows in Fig. 9). Indeed, many changes are seen among the magnetic lines which form a null point or saddle structures between AR 9082 and AR 9077, indicating large-scale magnetic reconnection there (see Tsuneta 1996).

In Figure 10, the extrapolated 3-D magnetic lines of force are superposed on the EIT base difference image showing the EUV dimming. All the dimming areas are, indeed, coincident with the footpoints of more than 10 sets of magnetic flux systems which have various spatial sizes and manifest different magnetic connectivity. This suggests again that multiple flux systems are involved in the process of the Bastille Day flare/CME event. It is noticed that many key dimming regions are seen at footpoints of interconnecting magnetic lines of force which are connected to the magnetic fields of AR 9077. This is indicative that magnetic fields in AR 9077 play some key role in triggering the eruption of the CME parent magnetic structure. The dimming at the footpoints of the sheared arcades of the transequatorial filament is clearly shown in the figure, which indicates the link between the transequatorial filament and the global CME.

5 DISCUSSION

We have identified a basic magnetic structure, an extended magnetic bipolar region (EBR) consisting of AR 9077 and two or three other smaller ARs, and a large area of enhanced magnetic network on the solar surface. The huge EBR and possibly other bipolar regions, inferred from EUV dimming and radio emission source in the low corona (displayed, respectively, in Figures 5, 6, and 7), seem to represent the basic pre-CME magnetic topology and to serve as the CME-parent magnetic structure. In a 3-D view, the central part of the EBR is the sheared magnetic arcades and a huge transequatorial filament underneath, which was channelling the north and south regions on the Sun.

Many observations show indications of the helical fields in filaments and magnetic field on either side of the filament channel (Schmieder, Malherbe & Raadu 1985; Vrsnak et al. 1988; Wang, Shi & Martin 1996). For the studied transequatorial filament, although the sheared magnetic arcades are successfully reconstructed from the non-linear force-free extrapolations, the magnetic fields in the transequatorial filament do not show up in the reconstructed 3-D structures. As described in Section 3, the Hα and EIT images revealed the helical structure of the filament during the filament activation and eruption. We will attempt to estimate whether or not the huge filament and its arcades can provide enough helicity to the CME. For a typical CME, it was believed to carry $10^{43}\,\mathrm{Mx}^2$ helicity in order of magnitude.

Unfortunately the nature of the magnetic fields in filaments and filament environment is still an open question (see a discussion by Wang et al. 2003). Rust & Kumar (1994) assumed that quiescent filament fields are suspended above the chromosphere with no connection to the underlying fields except at the two end-points of the long axis. They proposed a helical flux rope model of filaments. Martin & McAllister (1997), on the other hand, proposed a filament model in which the filament internal fields and the arcade fields are completely separated, and the internal fields come from the tightly packed magnetic fibers connected to the photospheric fields at the filament barbs. For simplicity, we adopt the Rust & Kumar model for the transequatorial filament, and use the Martin & McAllister model for the arcades. In our model, the filament is a helical flux rope and its arcades are a group of sheared flux loops like that shown by the 3-D reconstruction in Figure 7. Then the filament-arcade system has a total helicity

$$H_{\mathrm{total}} = H_{\mathrm{filament}} + H_{\mathrm{arcades}} + H_{\mathrm{mutual}}. \tag{1}$$

From Berger & Field (1984),

$$H_{\mathrm{filament}} = T{\Phi_{\mathrm{filament}}}^2, \tag{2}$$

and Φ can be roughly estimated as 10^{20} Mx, provided there was a 25 G field strength in the filament, and T here depends on the filament length and its helical nature. Since the filament was in unstable state for many hours before the eruption, the twist of the filament, T, can be as large as 2. Then, the helicity carried by the filament would be approximately $2{\times}10^{40}\,\mathrm{Mx}^2$, which is consistent with the estimate of Rust (2003) in order of magnitude for another large filament. Following Berger (1998) the helicity in the co-aligned sheared arcades is expressed as

$$H_{\mathrm{arcades}} = LS\hat{H}, \tag{3}$$

where $\hat{H}$ is the helicity of unit length, L the lateral length of the whole set of arcades, S the displacement of one footpoint in an arcade relative to the other footpoint, i.e., the shear of two footpoints. L is very close to the length of the filament and can be measured from the MDI magnetogram (see Fig. 8). The helicity in the arcades can be approximated as

$$H_{\mathrm{arcades}} = s{\Phi_{\mathrm{arcades}}}^2, \tag{4}$$

where s is the fraction of the average arcade shear to the lateral length of the whole set of the co-aligned arcades, and Φ_{arcades} is the total magnetic flux measured from arcade footpoints in one polarity. In our case, Φ_{arcades} measured $8{\times}10^{21}$. Taking s as 0.3 conservatively, then the total helicity is $1.9{\times}10^{43}\,\mathrm{Mx}^2$. The mutual helicity of the filament and arcades can be calculated by

$$H_{\mathrm{mutual}} = \frac{c}{\pi}\Phi_{\mathrm{filament}}\Phi_{\mathrm{arcades}}, \tag{5}$$

where c depends on the crossing angle determined by the distribution of the filament and arcades. Thus, the mutual helicity is estimated to be $8{\times}10^{41}\,\mathrm{Mx}^2$. The total helicity of the filament and arcade system is predominantly contributed by the long set of sheared magnetic arcades. It is on the order of magnitude of $10^{43}\,\mathrm{Mx}^2$.

Although this is only a rough estimation of total helicity, it reveals that for such a flux system with a filament and arcades the major part of helicity comes from the sheared arcades rather than from the twisted filament itself. A release of a fraction of the helicity in the overall field composition seems to be enough for the Bastille Day CMEs.

Remember, in the above estimation we have not fully taken into account the helicity from the strong and sheared magnetic fields in AR 9077. Wang (1996) estimated that for a rapidly growing AR, e.g., AR 6233, the rate of change of helicity was $2\times10^{39}\mathrm{Mx}^2\mathrm{s}^{-1}$ and the total helicity of this AR was $4\times10^{43}\mathrm{Mx}^2$. AR 9077 is much larger and much more complicated than AR 6233. Although no careful estimation on the helicity input from AR 9077 has been made, for such a super-active region it is quite safe to suggest that the total magnetic helicity in this AR should be very large, at least, many times of 10^{43} Mx^2. Moreover, AR 9077 is closely coupled with the large-scale magnetic structure (see the sigmoidal magnetic lines of force in the long filament arcades in Figs. 8 and 10). Therefore, it can not be fully excluded that AR 9077 provides a large fraction of its total helicity to the CME.

However, as argued by Wang et al. (2004), if we consider the fact that a CME is hosted by a much larger magnetic structure than an AR in spatial scale, it is not reasonable to search for the CME helicity source solely from the associated ARs. The large-scale field composition providing the birth of CMEs may contain enough helicity for CMEs as well as the free magnetic energy.

6 CONCLUSIONS

It is demonstrated that the Bastille Day flare/CME event is not a phenomenon of a single active region. Activation of a huge transequatorial filament is identified to precede the simultaneous filament eruption and flare in the source AR, NOAA AR 9077, and the full halo-CME in the high corona.

The observations of Hα, SOHO EIT, Yohkoh SXT, Nançay Radioheliogram and MDI magnetogram, and the 3-D extrapolations of magnetic lines of force suggest that a large-scale magnetic composition with many sets of interacting flux loops served as the CME parent magnetic structure. The transequatorial filament and its sheared arcade are the essential part in the pre-CME magnetic configuration. However, the large-scale multi-flux composition was initially removed in AR 9077. The opening of the overall flux systems in such a strong field region resulted in the explosive X5.7/3B flare, as suggested for more general cases by Švestka (2001). An estimation of the helicity found that the sheared magnetic arcades straddling the transequatorial filament provided the major part of the helicity in the flux system, and that could provide equivalent helicity to that carried by the CME. To search for the helicity source solely from the associated AR in this case is not a complete approach.

The case study sheds new light on our understanding of CME magnetism. At least for a more global CME, like the Bastille Day flare/CME event, a large-scale magnetic composition, e.g., an EBR consisting of a few ARs, a transequatorial filament and filament arcades, and a large area of enhanced magnetic network represent the pre-CME magnetic topology. The removal or the unwinding of the system may first take place in a magnetic complex region at active-region scale, like AR 9077 in this study. This tearing off of a magnetically complex region leads to flaring whereas the overall eruption of the large field composition causes CMEs. This scenario seems to outline the basic magnetism of CMEs and suggests a relationship between CMEs and active-region scale activity, e.g., flares and active-region filament eruptions.

A transequatorial filament with its extended, co-aligned sheared arcades appears to be a favorable configuration for global CMEs, particularly when the transequatorial filament is connected to a complex active region.

Like network and intranetwork fields are responsible for the ubiquitous activity on the quiet Sun, and like AR fields for flares and AR filament eruption, there must be a large-scale component in the hierarchy of solar magnetic fields that is responsible for the birth of global CMEs. The transequatorial filament and its sheared magnetic arcades described in this work may be one type of large-scale field component that hosts CMEs.

Since the recognition of the role of the transequatorial filament in the Bastille Day CME (Wang 2002; Wang et al. 2005), many tens of halo-CMEs have been identified that are associated with eruptive transequatorial filaments (Zhou et al. 2005). In future work we will study the general properties of the activity in transequatorial filaments and their associated CMEs.

Acknowledgements We would like thank Drs. Klein and Maia for the guidance in reducing the NRH data. The work is supported by the National Natural Science Foundation of China (NSFC, Grants 10233050 and 40274049) and National Key Basic Research Science Foundation (G2000078404). LKH is grateful for the Leverhulme Trust for the award of a Philip Leverhulme Prize. We are grateful to all members of the SOHO EIT, LASCO and MDI teams, as well as Huairou staff for providing the wonderful data. The authors are indebted to Nançay group for providing the very good radio observations. This CME catalog is generated and maintained by NASA and The Catholic University of America in cooperation with the Naval Research Laboratory. SOHO is a project of international cooperation between ESA and NASA.

References

Andrews M. D., 2001, Sol. Phys., 204, 179
Berger M. A., 1998, In: Wedd D., Rust D., Schmieder B., eds., New Perspectives on Solar Prominences, IAU COlloq. No. 167, ASP Conf. Series, 150, p.102
Berger M. A., Field G. A., 1984, J. Fluid Mech., 147, 133
Brueckner G. E., Howard R. A., Koomen M. J. et al., 1995, Sol. Phys., 162, 357
Chertok I. M., Fomichev V. V., Gnezdilov A. A. et al. 2001, Sol. Phys., 204, 139
Delaboudiniére J.-P., Artzner G. E., Brunaud J. et al., 1995, Sol. Phys., 162, 291
Deng Y., Wang J., Yan Y. et al., 2001, Sol. Phys., 204, 11
DeVore C. R., 2000, ApJ, 539, 944
Green L. M., Lopez Fuentes M. C., Mandrini C. H. et al., 2002, Sol. Phys., 208, 43
Harra L. K., Sterling A. C., 2003, ApJ, 587, 429
Harrison R. A., 1990, Sol. Phys., 126, 185
Harvey K. L., Martin S. F., 1973, Sol. Phys., 32, 389
Liu Y., Zhang H., 2001, A&A, 372, 1019
Liu Y., Zhang H., 2002, A&A, 386, 640
Maia D., Pick M., Hawkins S. E. III, et al., 2001, Sol. Phys., 204, 197
Martin S. F., 1988, Sol. Phys., 117, 243
Martin S. F., McAllister A. H., 1997 In: Crooker N., Joselyn J. A., Feynman J. eds., Coronal Mass Ejections, Geophys. Monograph 99, American Geophys. Union, Washington, D. C., p.127
Masuda S., Kosugi T., Hudson H. S., 2001, Sol. Phys., 204, 55
Parker E. N., 2001, ChJAA, 1, 99
Raeder J., Wang Y. L., Fuller-Rowell T. J. et al., 2001, Sol. Phys., 204, 323
Reiner M. J., Kaiser M. L., Karlicky M. et al., 2001, Sol. Phys., 204, 121
Rust D. W., Kumar A., 1994, Sol. Phys., 155, 69
Rust D. M., 2003, Adv. Space Res., 32, 1895
Scherrer P. H., Bogart R. S., Bush R. I. et al., 1995, Sol. Phys., 162, 129
Schmieder B., Malherbe J. M., Raadu M. A., 1985, A&A, 142, 249
Švestka Z., 2001, Space Sci. Rev., 95, 135
Tian L., Wang J., Wu D., 2002, Sol. Phys., 209, 375
Tsuneta S., Acton L., Bruner M. et al., 1991, Sol. Phys., 136, 37
Tsuneta S., 1996, ApJ, 456, L63
Vrsnak B., Ruzdjak V., Brajsa R. et al., 1988, Sol. Phys., 116, 45
Wang H., Yan H., Sakurai T., 2001, Sol. Phys., 201, 323
Wang J., Shi Z., Martin S. F., 1996, A&A, 316, 201
Wang J. X., Li W., Denker C. et al., 2000, ApJ, 530, 1071
Wang J., 2002, In: Henoux J.-C., Fang C., Vilmer N. eds., Understanding Solar Active Phenomenoa, Beijing: Inter. Sci. Publ. & Worl Publ., p.145
Wang J. X., Zhou G. P., Wang Y. M. et al., 2003, Sol. Phys., 216, 143
Wang J. X., Zhou G. P., Zhang J., 2004, ApJ, 615, 1021
Wang J. X., Zhou G. P., Wen Y. Y. et al., 2005, In: Dere K., Wang J. X., Yan Y. H., eds., Coronal and Stellar Mass Ejections, Proc. IAU Symp., 226, Cambridge Univ. Press, p.135
Wen Y. Y., Wang J. X. 2005, In: Dere K., Wang J. X., Yan Y. Y., eds., Coronal and Stellar Mass Ejections, Proc. IAU Symp., 226, Cambridge: Cambridge Univ. Press, p.141
Zhang J., Wang J. X., Lee C.-Y. et al., 2002, Sol. Phys., 194, 59
Zhang J., Wang J. X., Deng Y. et al., 2001, ApJ, 548, L99
Zhou G. P., Wang J., Zhang J., 2005, A&A, 445, 1133